Supplementary figure 1

A

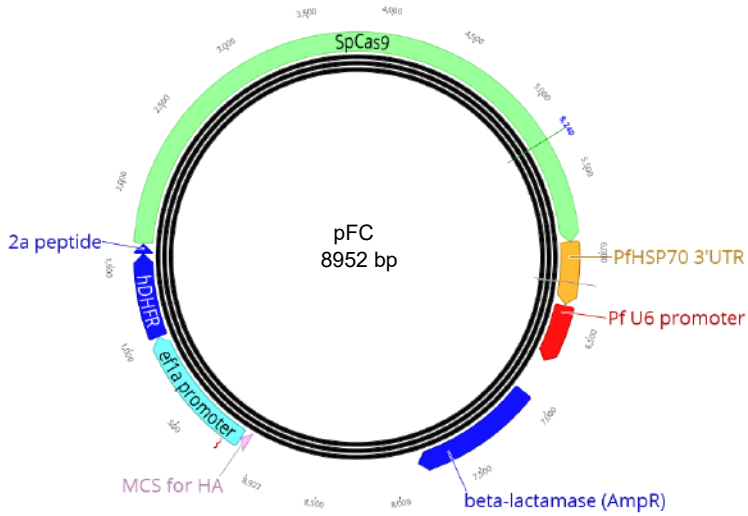

B

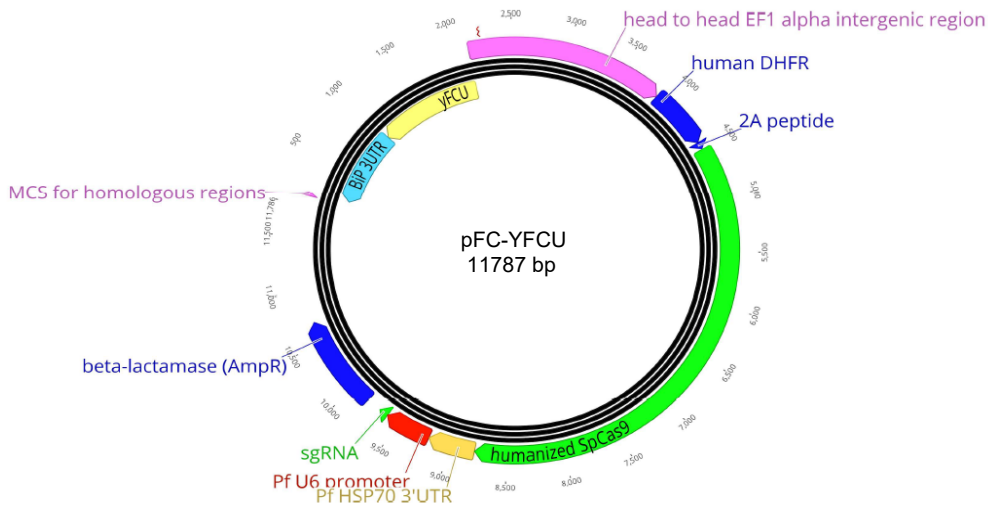

Supplementary Figure 1: (A) pFC plasmid map (B) pFC-yFCU plasmid map

Supplementary figure 2

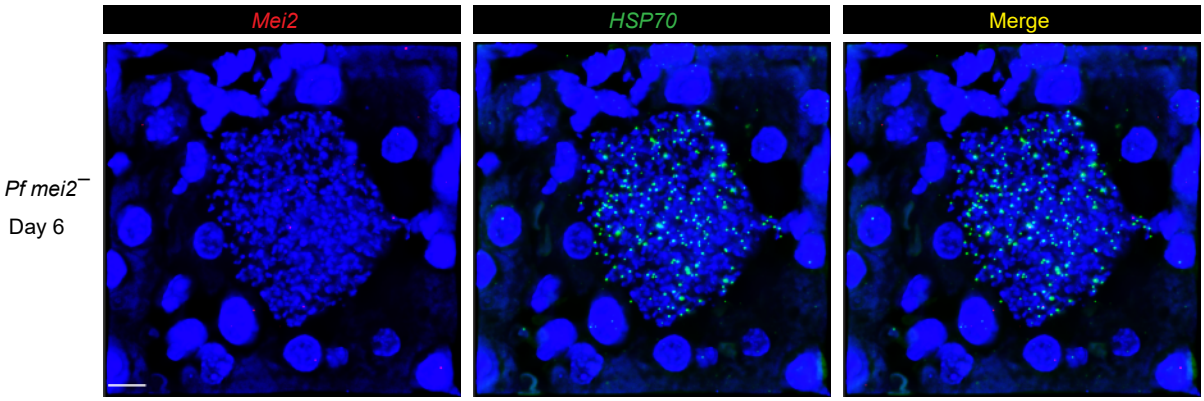

Supplementary Figure 2: Lack of expression of *Mei2* in *Pf mei2*$^{-}$ liver stage parasites by RNAscope. Specificity of the *Pf Mei2* probe and lack of expression of *Mei2* was confirmed by performing RNAscope on infected liver sections of *Pf mei2*$^{-}$ on day 6 post infection. Probes targeted *Mei2* (red) and *HSP70* (green). Scale bar is 7 µm.

Supplementary figure 3

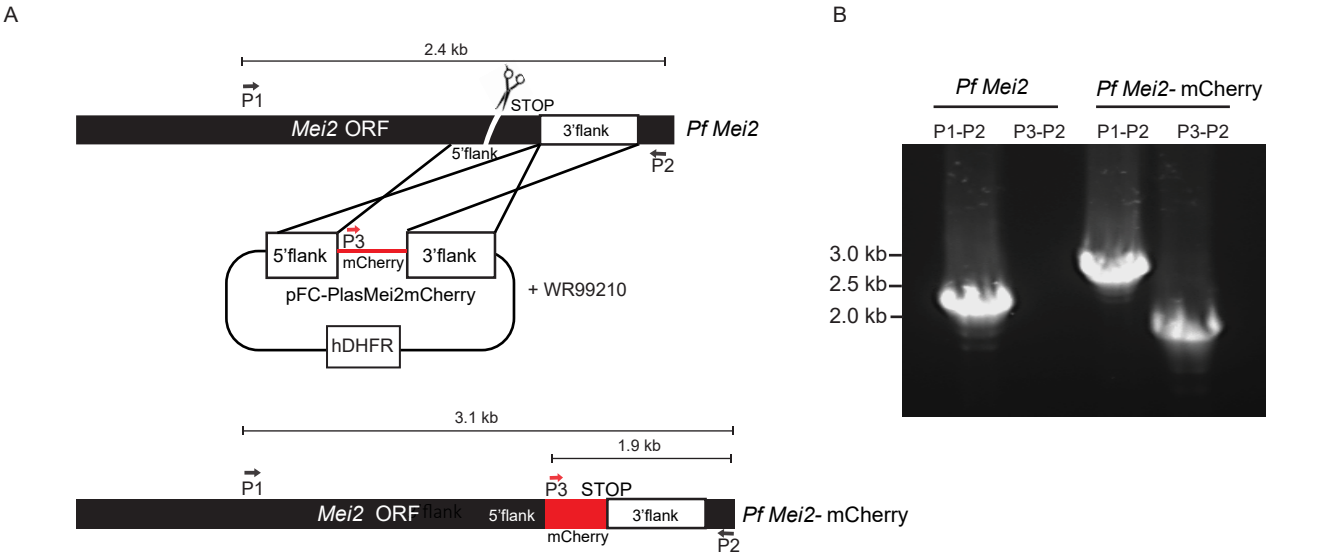

Supplementary Figure 3: Generation of marker free *Plasmodium falciparum Mei2* mCherry epitope tagged parasite line. (A) The schematic depicts the generation of the *Pf Mei2*-mCherry parasites by CRISPR/Cas9-mediated gene editing (upper panel). Primers used to verify the integration are indicated and the sizes of the PCR products are shown in bases (lower panel). (B) Agarose gel electrophoresis shows the PCR products corresponding to the correct insertion of the mCherry cassette in the *Pf Mei2* locus.

Supplementary figure 4

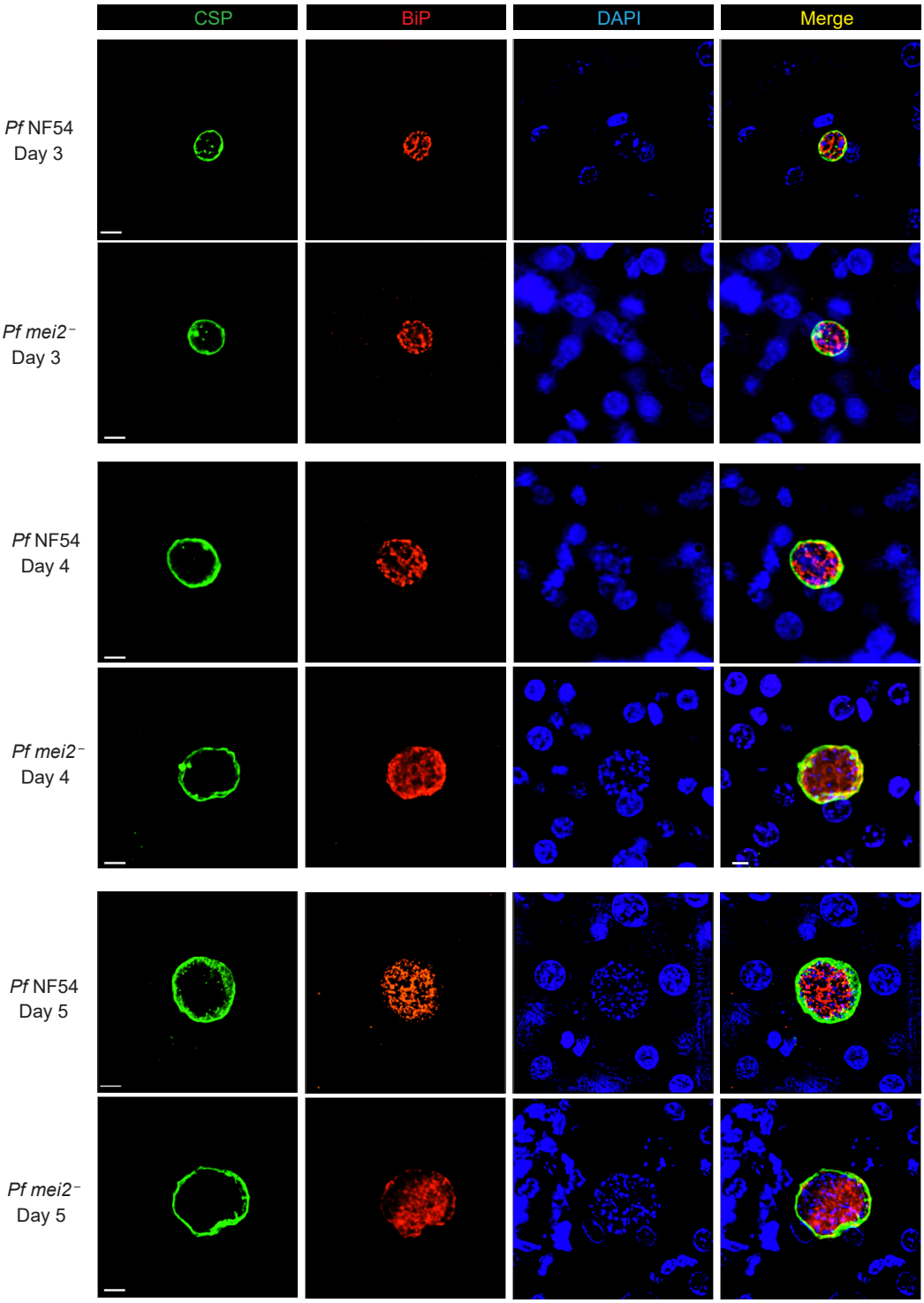

Supplementary Figure 4: *Pf mei2*⁻ liver stage development is normal from early- to mid-liver stage. Tissue sections were prepared from FRG NOD huHep mice infected with *Pf* NF54 and *Pf mei2*⁻ sporozoites on days 3, 4 and 5 of liver stage development and analyzed by IFA. Parasites were detected with antibodies to CSP (green) which localizes to the parasite plasma membrane (PPM) and BiP (red) which localizes to the endoplasmic reticulum. DAPI (blue) was used to label DNA. *Pf mei2*⁻ liver stages display normal morphology at this early-to-mid liver stage development. Scale bar is 7 μm.

Supplementary figure 5

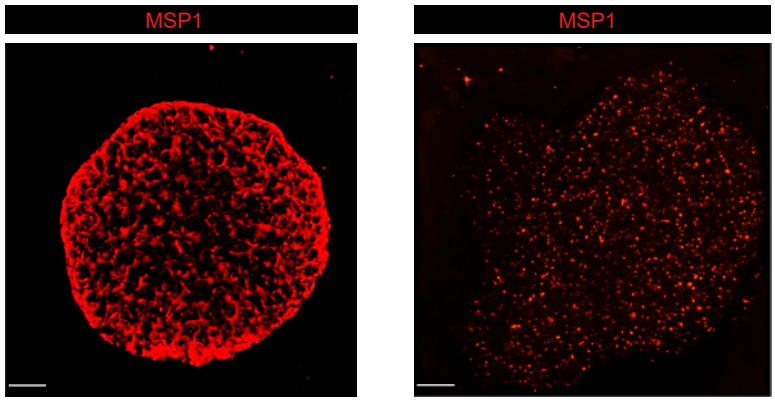

Supplementary Figure 5: *Pf mei2*$^{-}$ does not form exo-erythrocytic merozoites. IFA for MSP-1 (red) in *Pf* NF54 (left) and *Pf mei2*$^{-}$ (right) display extensive membrane staining in *Pf* NF54, but diffused staining in *Pf mei2*$^{-}$, suggesting a lack of merozoite formation. Scale bar is 7 µm.

Supplementary figure 6

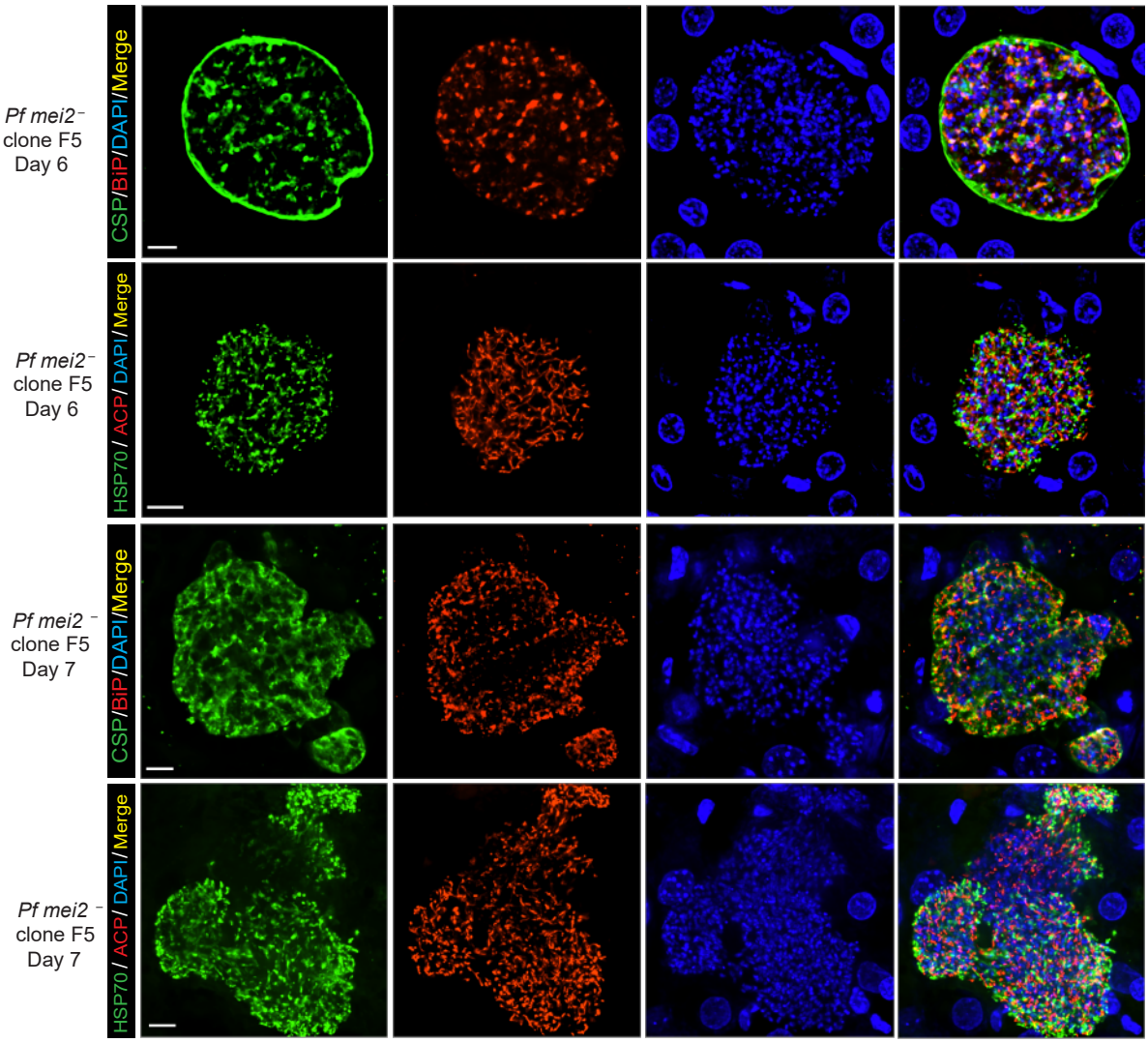

Supplementary Figure 6: *Pf mei2*⁻ liver stage development is similar for clones F2 and F5. Tissue sections were prepared from FRG NOD huHep mice infected with *Pf mei2*⁻ sporozoites from clone F5 and analyzed by IFA on days 6 and 7 post infection. IFA was used to localize the parasite plasma membrane (CSP), ER (endoplasmic reticulum), apicoplast (ACP) and mitochondria (mHSP70). DNA was labeled with DAPI. Defects in liver stage differentiation are similar for *Pf mei2*⁻ clone F5 on days 6 and 7 with lack of cytomere formation, aberrant organellar segregation and absence of exo-erythrocytic merozoites. Scale bar is 7µm.

Supplementary figure 7

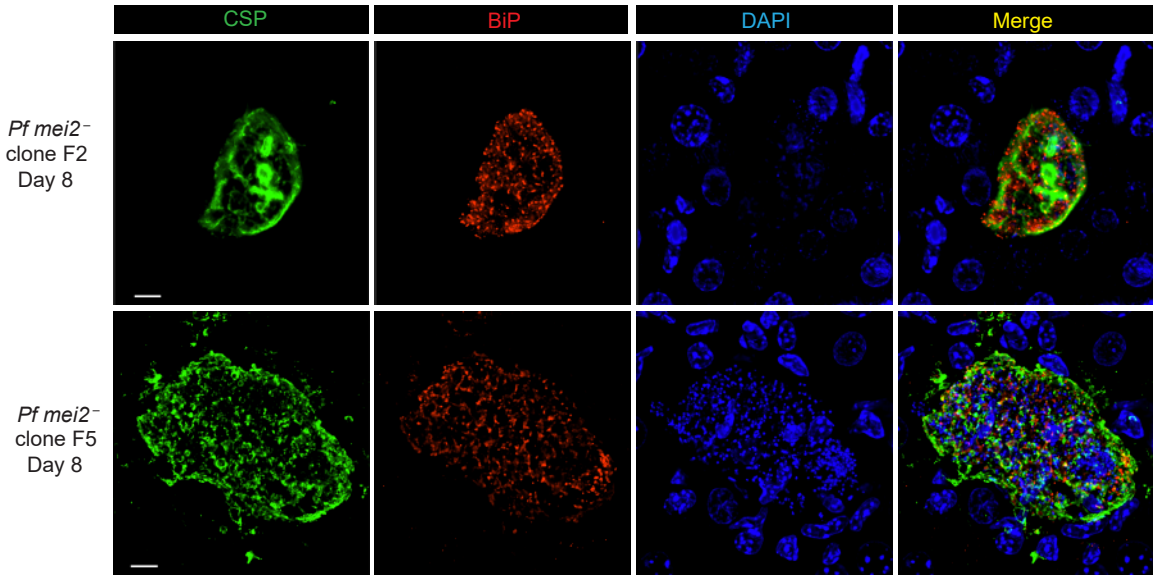

Supplementary Figure 7: *Pf mei2*$^{-}$ liver stage parasites on day 8 do not undergo further differentiation. Tissue sections were prepared from FRG NOD huHep mice infected with sporozoites from *Pf mei2*$^{-}$ clones F2 and F5 on day 8 and analyzed by IFA. IFA was used to localize the parasite plasma membrane (CSP) and ER (endoplasmic reticulum). DNA was labeled with DAPI. No viable parasites were detected on day 8. Scale bar is 7 µm.

Supplementary figure 8

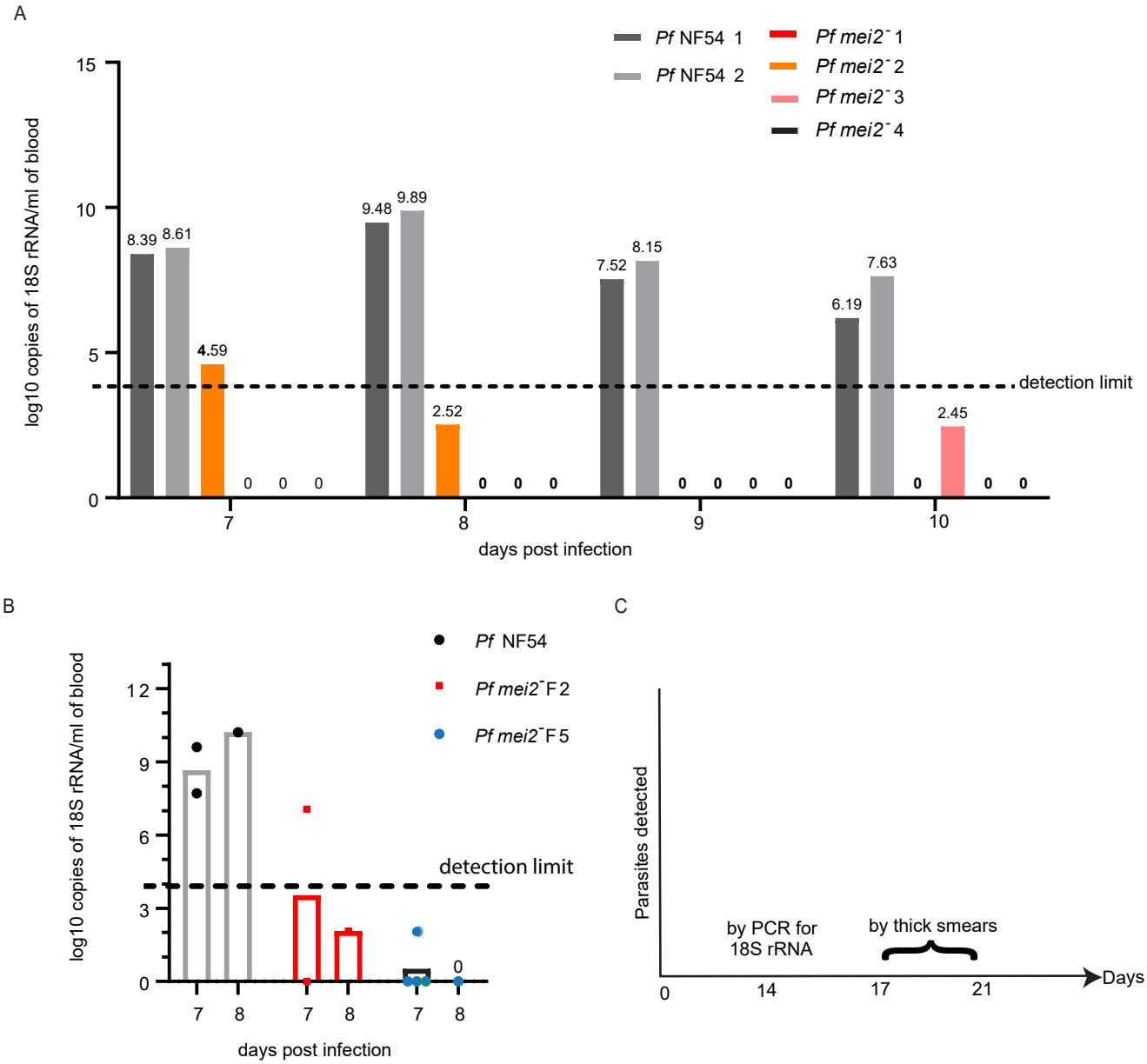

Supplementary Figure 8: qRT-PCR for *Pf* 18s rRNA from whole mouse blood indicated severe attenuation of *Pf mei2*⁻. (A) Mice were infected as described in Figure 6A. One million *Pf* NF54 sporozoites were injected i.v. into two FRG huHep mice and *Pf mei2*⁻ sporozoites were injected i.v. into 4 FRG huHep mice. 18S rRNA qRT-PCR was performed from 50 µl of whole mouse blood from days 7 through 10 post infection. 18S rRNA qRT-PCR signal is detected in the two mice from days 7 through 10. For *Pf mei2*⁻ infected mice, mouse 1 displays a low positivity by 18S rRNA qRT-PCR only on day 7 and was negative by 18S rRNA qRT-PCR from days 8 - 10. The other three mice remained negative from days 7 through 10. (B) Mice were infected as described in Figure 6B. One million *Pf* NF54 and one million *Pf mei2*⁻ sporozoites from clones F2 and F5 were injected i.v. into two, two, and four FRG NOD huHep mice respectively. 18S rRNA qRT-PCR was performed from 50 µl of whole mouse blood from all 6 mice on day 7 and from 1 mouse per group also on day 8. Both mice infected with NF54 were positive by 18S rRNA qRT-PCR on day 7, out of which one was sacrificed on day 7. The second mouse that was sacrificed on day 8, was also positive by 18S rRNA qRT-PCR on day 8. One mouse infected with *Pf mei2*⁻ clone F2 was positive on day 7, while the other mouse was negative. The second mouse was also negative by 18S rRNA qRT-PCR on day 8. All mice infected with *Pf mei2*⁻ clone F5 were negative on both day 7 and 8. (C) Timeline for when *Pf mei2*⁻ clones were detected by thick smear after limiting dilution cloning of parasites at 0.1 parasites/ml from mixed populations of recombinant *Pf mei2*⁻ post transfection with pFC-PlasMei2. PCR for 18S rRNA was positive by Day 14 and parasites were detected on thick smears between days 17 and 21. The inability to recover *Pf mei2*⁻ blood stages after liver-to-blood stage transition in FRG huHep/FRG NOD huHep mice is not due to impaired blood stage growth of *Pf mei2*⁻ when seeded at low densities.

Materials and Methods

Mice

FRG and FRG NOD huHep mice (both male and female, >4 months of age) were purchased from Yecuris, Inc. Repopulation of human hepatocytes was confirmed by measuring human serum albumin levels, and only animals with human serum albumin levels >4 mg/mL were used as previously described (1).

Generation of *Pf mei2*$^{-}$ and *Pf mei2*–mCherry

All oligonucleotides used for generation and analysis of transgenic parasites are delineated in Supplementary Table 1. *Pf mei2*$^{-}$ was generated by CRISPR/Cas9-mediated gene editing using the pFC plasmid, which was designed in a manner similar to the pYC plasmid previously reported (2). Briefly, the pFC plasmid includes the *Pf* U6 promoter driving expression of a sgRNA cassette, the *Pf* EF1α promoter driving the positive selection marker; *hDHFR* and codon optimized *S. pyogenes Cas9* as a bi-cistronic transcript separated by a 2A viral skip peptide, and a multiple cloning site for cloning the repair templates for recombination (Supplementary Figure 1A). The pFC-PlasMei2 plasmid included the homology arms flanking the upstream and downstream regions of the *Pf Mei2,* cloned into the multiple cloning site of the pFC plasmid between the SalI and NotI sites. Two different guides were used to target the *Pf Mei2* locus, *Mei2* Guide 1 and 2, to generate the plasmids pFC-plasMei2-G1 and pFC-plasMei2-G2. 5% sorbitol synchronized *Pf* NF54 ring stage parasites were co-transfected with 100µg of pFC-PlasMei2-G1 and pFC-PlasMei2-G2 by electroporation at 0.31 kV and 950 µF using a BioRad Gene Pulser (BioRad, Hercules, CA) as

previously described (3). For positive selection, these parasites were treated with 8 nM WR99210 (WR; Jacobus Pharmaceuticals, Princeton, NJ) 24 hours post transfection for 5 days, followed by media changes without any drug until parasites were detected on thick smears (17-21 days). Recombinant parasites were screened by PCR genotyping and cloned by limiting dilution.

For generation of marker free *Pf mei2*$^{-}$ that do not retain any extraneous DNA, the pFC-yFCU plasmid was generated by modifying the pFC plasmid (Supplementary figure 1B). The truncated *Pf* EF1α promoter was replaced by the complete intergenic region between the two *Pf* EF1α genes to generate a bidirectional promoter. The negative selection marker, *yFCU* was cloned at one end of the promoter, and the positive selection marker *hDHFR*, was cloned at the opposite end. The same donor flanking arms were used as for the pFC-PlasMei2 construct to generate the pFC-yFCU-PlasMei2 plasmid. Three different guides were used to target the *Pf Mei2* locus, *Mei2* Guide 1, 2 and 3 to generate the plasmids pFC-yFCU-PlasMei2-G1 through G3. Two independent transfections were carried out using the protocol mentioned above. In transfection 1, 100µg of pFC-yFCU-PlasMei2-G1 and pFC-yFCU-PlasMei2-G2 plasmids were co-transfected, while in transfection 2, pFC-yFCU-PlasMei2-G1 and pFC-yFCU-PlasMei2-G3 were co-transfected. Transfected parasites were positively selected as mentioned above. Once parasites were visible on thin blood smears (around day 15), parasites were put through two rounds of negative selection pressure with 5FC (1 µM) for 7 days each and cloned by limiting dilution.

Pf Mei2-mCherry parasites were generated via CRISPR/Cas9-mediated gene editing by transfecting wildtype *Pf* NF54 with 100µg of the pFC-PlasMei2mCherry plasmid in the pFC plasmid backbone (Supplementary Figure 1A). The 5'homology arm was amplified from within the *Pf Mei2* open reading frame with non-synonymous mutations introduced in the guide. The

3’homology arm was the same as used in the pFC-PlasmMei2 plasmid. Transfected parasites were positively selected as mentioned above, recombinant parasites were screened up PCR and cloned by limiting dilution.

Parasite cloning by limiting dilution

Recombinant parasites were screened by limiting dilution as previously described (3). Two clones for *Pf mei2*$^{-}$; F2 and F5 were used for further phenotypic analysis.

Southern Blotting

Recombinant clones for *Pf mei2*$^{-}$; F2 and F5, were verified for the correct integration pattern using Southern blot using the Roche kit according to the manufacturer’s instructions and as previously described (3). *Pf* NF54 and *Pf mei2*$^{-}$ genomic DNA was digested with XhoI, AflII, and HindIII. The 3’*Mei2* was amplified from *Pf* NF54 genomic DNA using primers, 3'Plasmei2probe_F (5’CACATTATACATATTTGATTAG, sense) and 3'Plasmei2probe_R (CCTGTCTTACATAAAGCCATAGAGC, antisense).

Mosquito infections and sporozoite production

Asexual blood stage cultures were maintained in RPMI 1640 (25 mM HEPES, 2 mM L-glutamine) supplemented with 50 μM hypoxanthine plus 10% human serum and subcultured in 5% O+ blood (Valley Biomedical, VA). Mature gametocytes were generated as described (3–5). Oocyst prevalence was checked on day 7 – 9 post feed by microdissecting approximately 12 midguts per

cage. Sporozoite numbers were detected by dissecting and grinding salivary glands in Schneider′s Insect Medium (Sigma) on days 14 – 18 post feed. These sporozoites were used for i.v. injections into FRG huHep mice.

FRG huHep mouse infections and liver stage-to-blood stage transition

FRG huHep and FRG NOD huHep mice were purchased from Yecuris Corporation and exhibited primary hepatocyte repopulation levels of at least 70% based on the serum levels for human albumin. Animals were cycled on 8 mg/L of NTBC once a month for 4 days to maintain hepatocyte chimerism. Mice were taken off NTBC 3 weeks prior to and during experimentation.

Analyzing the liver stage-to-blood stage transition in FRG huHep mice

FRG huHep mice were infected with 1 million sporozoites of *Pf* NF54 or *Pf mei2*$^{-}$ clone F2 by i.v. injection. Mice were injected with 100 µl of Chlodronate Liposomes (CloLip; Clophosome®-A, FormuMax) and 100 µl of Cyclophosphamide (Sigma Aldrich, St. Louis, MO, USA) by i.p. injection on days 1, 5 and 8 post infection to clear mouse macrophages and neutrophils. To transition parasites from the liver stage-to-blood stage, mice were injected with 400 µl of human RBCs at 70% hematocrit by i.v. injection on days 6 and 7 and by i.p. injection on day 8. 50 µl of blood was removed for 18S rRNA qRT-PCR analysis from days 7 through 10. 500µl of blood was drawn by retro-orbital bleeds and transferred to in vitro culture on day 7. Mice were exsanguinated on day 10 and blood was transferred to in vitro culture.

Analyzing the liver stage-to-blood stage transition in FRG NOD huHep mice

FRG NOD huHep mice were infected with 1 million sporozoites of *Pf* NF54 and *Pf mei2*$^{-}$ clones F2 and F5. Mice were injected with 400 µl of 70% human RBCs on days 6 and 7. 50 µl of blood was removed for 18S rRNA qRT-PCR on day 7 and/or day 8. The mice were either exsanguinated on day 7 or on day 8 and the blood was transferred to in vitro culture.

In vitro culture of transitioned mouse blood

Blood was removed in sterile conditions by cardiac puncture on days 7, 8 or 10 post infection and processed as previously described (4). Fresh media was replaced daily, and cultures were analyzed every 2-3 days by thick smear for presence of parasites. Samples for 18S rRNA qRT-PCR were removed every 5-7 days.

18S rRNA qRT-PCR quantification of parasite load

For parasite liver stage infection analysis, livers were harvested on days 6 and 7 post infection. Liver sections were added to Trizol reagent (Invitrogen), homogenized and RNA was extracted using the RNAeasy Qiagen purification kit (Qiagen). 18S rRNA qRT-PCR analysis was carried out as previously reported using a pan-*Plasmodium* probe (5,6). The 18S RNA values for *Pf* NF54 sporozoite infected livers on days 6, 7 and 8 were used as controls to compare the liver load for both *Pf mei2*$^{-}$ liver stage load on the same time points.

For quantification of 18S rRNA from mouse blood, blood was added to NucliSENS lysis buffer (bioMérieux, Marcy-l'Étoile, France) and frozen immediately at -80°C. The samples were processed and analyzed for presence of 18S rRNA as previously described (7).

Immunofluorescence assay of liver stage parasites

FRG huHep mice were injected with 1 million sporozoites of *Pf* NF54 or *Pf mei2*$^{-}$ sporozoites. Livers were harvested on days 3 through 8 post infection, fixed in 4% (vol/vol) paraformaldehyde (PFA, Alfa Aesar) in 1X PBS and processed for IFA as previously described (8). Primary antibodies used included *Pf* CSP clone 2A10 (1:500), *P. yoelii* BiP polyclonal (1:1000), *P. yoelii* ACP (1:500), *P. vivax* mHSP70 (1:1000) and *Pf* MSP-1 clone 12.10 (1:500, European Malaria Reagent Repository), mCherry clone 16D7 (1:500, Thermo Scientific).

Phenotypic analysis of liver stage parasites

Deconvolution and image analysis

All images were acquired using Olympus 1x70 DeltaVision deconvolution microscopy. All immunofluorescence images were deconvolved using Huygens Essential deconvolution software and analyzed using Imaris 9.2.1 software.

Analysis of parasite liver stage area

The IFA using the CSP antibody was used to measure the area of liver stage parasites. The parasite was assumed to be an ellipse and area was calculated from its longest (a) and shortest (b) circumferential diameter (πab).

Quantification of day 7 liver stage parasite DNA centers

DNA center quantification was performed using Imaris 9.3.1 software. Deconvolved images of day 7 liver stages for NF54 and *Pf mei2*$^{-}$ stained with CSP and DAPI were used for quantification. CSP staining was used to mark the outline of the liver stage parasite using the "surface" feature. Within this outline, the number and volume of DAPI centers were analyzed using the "spots" feature

Quantification of merosome-like structures

IFAs of day 7 liver stage parasites from NF54 and *Pf mei2*$^{-}$ using antibodies to CSP and BiP alongside DAPI were used to assess extrusome formation.

RNA fluorescent *in situ* hybridization using RNAscope technology

RNA in situ hybridization was performed using RNAscope Multiplex Fluorescent Assay v2 (Advanced Cell Diagnostics) to detect *Pf Mei2* transcript using manufacturer's instructions and as previously described (9). Target probes were designed for *Pf Mei2* and *Pf HSP70*. Binding of probes to the target locus results in formation of a Z configuration which enables amplification of signal and binding of target dyes as previously reported (10). The *Pf Mei2* probe was detected using the dye Opal 670 (Akoya Biosciences) and the Cy5 filter. The *Pf HSP70* probe was detected using the dye Opal 620 (Akoya Biosciences) and the mCherry filter.

1. Azuma H, Paulk N, Ranade A, Dorrell C, Al-dhalimy M. Robust expansion of human hepatocytes in Fah-/-/Rag2-/ − /Il2rg−/−mice. *Nat Biotechnol*. 2007;25(8):903-910. doi:10.1038/nbt1326.Robust

2. Zhang C, Xiao B, Jiang Y. Efficient Editing of Malaria Parasite Genome Using the CRISPR / Cas9. *MBio*. 2014;5(4):1-9. doi:10.1128/mBio.01414-14.Editor

3. Mikolajczak S a, Lakshmanan V, Fishbaugher M, et al. A next-generation genetically attenuated Plasmodium falciparum parasite created by triple gene deletion. *Mol Ther*. 2014;22(9):1707-1715. doi:10.1038/mt.2014.85

4. Vaughan AM, Mikolajczak SA, Wilson EM, et al. Technical advance Complete Plasmodium falciparum liver-stage development in liver-chimeric mice. *J Clin Invest*. 2012;122(10). doi:10.1172/JCI62684.3618

5. Flannery EL, Foquet L, Chuenchob V, et al. Assessing drug efficacy against Plasmodium falciparum liver stages in vivo. *JCI Insight*. 2018;3(1). doi:10.1172/jci.insight.92587

6. Sack BK, Mikolajczak SA, Fishbaugher M, et al. Humoral protection against mosquito bite-transmitted Plasmodium falciparum infection in humanized mice. *npj Vaccines*. 2017;2(1):1-10. doi:10.1038/s41541-017-0028-2

7. Seilie AM, Chang M, Hanron AE, et al. Beyond blood smears: Qualification of plasmodium 18s rrna as a biomarker for controlled human malaria infections. *Am J Trop Med Hyg*. 2019;100(6):1466-1476. doi:10.4269/ajtmh.19-0094

8. Dankwa DA, Davis MJ, Kappe SHI, Vaughan AM. A Plasmodium yoelii Mei2-like RNA binding protein is essential for completion of liver stage schizogony. *Infect Immun*.

2016;84(5):1336-1345. doi:10.1128/IAI.01417-15

9. Fisher BS, Green RR, Brown RR, et al. Liver macrophage-associated inflammation correlates with SIV burden and is substantially reduced following cART. *PLoS Pathog*. 2018;14(2):e1006871.

10. Wang F, Flanagan J, Su N, et al. RNAscope: A novel in situ RNA analysis platform for formalin-fixed, paraffin-embedded tissues. *J Mol Diagnostics*. 2012;14(1):22-29. doi:10.1016/j.jmoldx.2011.08.002